The Utility of Radium as a Tracer in a River-dominated System

Principal Investigator: Josianne Haag[1]

[1] College of Fisheries and Ocean Sciences, University of Alaska Fairbanks

October 2022
Final Reports
OCS Study BOEM 2022-046

BOEM Bureau of Ocean Energy Management

UAF University of Alaska Fairbanks

Contact Information:

uaf-cmi@alaska.edu
https://www.uaf.edu/cfos/research/cmi

This study was funded by the U.S. Department of the Interior, Bureau of Ocean Energy Management Alaska OCS Region (Cooperative Agreement M20AC10016) and the University of Alaska Fairbanks. This report, BOEM 2022-046, is available through the Coastal Marine Institute and electronically from https://www.boem.gov/akpubs.

TABLE OF CONTENTS

LIST OF FIGURES

LIST OF TABLES

ABSTRACT

This project examined the utility of radium-based approaches in Kachemak Bay in southcentral Alaska. Radium is a common tracer of groundwater nutrient inputs to the coastal ocean and is used to expand our understanding of coastal ocean ecosystems. Radium samples were taken from Kachemak Bay and six rivers that discharge into the bay. Results show strong correlations (r^2> 0.75) between radium isotopes and watershed characteristics as determined from satellite imagery of the region, including elevation, area, slope, and land type (forest, glacier, wetland, and barren land). Exchangeable radium makes up the greatest portion of the radium budget in a river and can desorb from riverine suspended solids through cation exchange in seawater and potentially masking groundwater radium signals. In fact, in this study, groundwater radium was only detected in bays and coastlines with minimal river discharge. The concentration of radium in offshore waters is depleted by groundwater and river inputs; therefore, short-lived radium can only be used as a tracer close to its source.

INTRODUCTION

Background

Submarine groundwater discharge (SGD) is an essential driver of biogeochemical cycles, though it is often overlooked in nearshore studies due to the difficulties in its estimation. Positive impacts of SGD include the enhancement of coral calcification, primary productivity, fisheries, denitrification, and pollutant attenuation. However, SGD can also negatively alter a coastal ecosystem by provoking eutrophication, algal blooms, deoxygenation, and localized ocean acidification (Santos et al., 2021). Unfortunately, there is a lack of SGD research in areas with extreme tidal ranges. High rates of SGD are expected in Kachemak Bay, an arm of Cook Inlet in southcentral Alaska. Cook Inlet has some of the world's greatest tidal ranges (Archer, 2013) and soft permeable sediment on most of the seafloor (Oey et al., 2007). Furthermore, SGD in Alaska can rival river fluxes as a nutrient source across the entire Northern Gulf of Alaska (NGA) (Lecher et al., 2016b).

Naturally occurring radium (Ra) isotopes are well established as ideal groundwater tracers in coastal systems and have been used in a wide range of nearshore studies for nearly three decades. The four naturally occurring Ra isotopes decay at different rates (^{223}Ra, $t_{1/2}$ = 11.4 days; ^{224}Ra, $t_{1/2}$ = 3.63 days; ^{226}Ra, $t_{1/2}$ = 1600 years; ^{228}Ra, $t_{1/2}$ = 5.75 years) allowing for the study of processes at various oceanographic timescales. Ra is a land-derived element that desorbs from sediment at land-ocean boundaries through cation exchange, a process that occurs in saline water (Hancock et al., 2000); therefore, Ra can be used as a tracer of terrestrial water in the ocean. The groundwater concentration of Ra is determined by the concentration of its parental isotope, uranium, in the aquifer. Ra is typically one to three times more concentrated in groundwater than in seawater (Moore, 2000; Garcia-Orellana et al., 2021). The concentration of ^{224}Ra in groundwater in the NGA is two to three times greater than seawater at a mudflat (Kelley et al., 2022) and an order of magnitude greater than at a rocky beach (Lecher et al., 2016a).

Kachemak Bay is one of the most intensely studied fjord-type estuaries in Alaska and has markedly different geology on either side of the bay (Bradley et al., 1999). Sedimentary rock of non-marine origin north of the bay is called the Peninsular Terrane (Croff et al., 1977). The Chugach Terrane, a composite terrane south of the bay, was created through four periods of accretion of the oceanic plate during the Mesozoic (Pavlis et al., 2007). It is dominated by marine sedimentary rock with many Paleogene igneous intrusions (Plafker et al., 1989). The bedrock from the two distinct terranes of Kachemak Bay could contain different concentrations of uranium, which will control the concentration of Ra in groundwater.

The quaternary surficial deposits overlying much of the bedrock in Kachemak Bay form the primary aquifer through which groundwater flows. This unconsolidated material is composed of fluvial floodplain, colluvial, glacial, alluvial fan, landslide, and swamp deposits (Bradley et al., 1999). Schmoll et al. (1984) found that the primary aquifer in the bay is composed of unconsolidated glacially-derived sediment. The groundwater from alluvial aquifers is typically calcium-bicarbonate or calcium-magnesium bicarbonate facies (Sharp, 1988). This chemistry is present in five major rivers feeding into Kachemak Bay from the south shore (Jordan Jenckes,

pers. comm.). Due to the fining-upward substratum of alluvial aquifers in this region (Dickinson and Campbell, 1978), a larger grain size at depth corresponds to higher permeability (Sharp, 1984) and creates a "skin effect" where the bed of a river running over the aquifer has less permeability than the alluvial aquifer (Sharp, 1984), potentially confining the groundwater.

A Ra-based SGD estimate requires distinguishing the concentration of Ra in groundwater from that in the background seawater. If the river Ra flux into Kachemak Bay is too great, it could overwhelm the groundwater Ra flux. The Ra adsorbed to riverine suspended solids could be released through cation exchange when the fresh river water reaches the saline estuary. This fraction is called exchangeable Ra. The Ra locked into the crystal lattice of the suspended solids does not desorb, which limits the exchangeable Ra and allows a threshold to be reached (Hancock and Murray, 1996; Hancock et al., 2000). This threshold is reached at a salinity of 15, at which time the full desorption of exchangeable Ra can increase the river Ra concentration six-fold (Kelley et al., 2022). The groundwater Ra concentration is still six times greater than the river Ra budget including exchangeable Ra; however, in a river-dominated system, the Ra flux from the rivers may confound accurate estimation of groundwater Ra flux.

The major rivers in Kachemak Bay flow through the Chugach Terrane on the south side of the bay and span a gradient from glacially-dominated to non-glacial watersheds. The differences between Ra concentration across the rivers will likely be controlled by watershed characteristics. The retreating glaciers in the watersheds of many of these rivers control the hydrogeology of the aquifers and the chemical components of the rivers. During spring melt, the rising river stage will recharge the alluvial aquifers and the water in bank storage. During the summer, when the river stage declines, the water in bank storage will discharge into the rivers (Jordan Jenckes pers. comm.). Recharge from bedrock aquifers into rivers is less pronounced due to the higher permeability of the alluvium (Sharp, 1984). Additionally, the area in front of the glacial terminus (the proglacial zone) freezes, thaws, and dries on an annual basis, which results in freshly comminuted silt-sized glacial flour through mechanical erosion (Tranter 1982). Chemical erosion, the weathering process in which elements from the bedrock below the glacier are dissolved into the river water, has high rates of erosion with basalt (Tranter 2003), which is the primary bedrock in the Chugach Terrane where these glacially fed rivers are located. The Ra contributed to the river water by mechanical and chemical erosion can mask the groundwater Ra signal. This project provides an understanding of the utility of Ra-based approaches in a river-dominated system.

Objectives

Objective 1: Assess the relative importance of Ra inputs from rivers and groundwater to determine the viability of using Ra as a tracer.

> Hypothesis 1a: The desorption of exchangeable Ra from riverine suspended solids masks the groundwater Ra signal.
>
> Hypothesis 1b: Rivers with greater percent glaciation have greater mechanical weathering of bedrock, resulting in more exchangeable Ra.

Objective 2: Identify the major physiochemical controls over surface macronutrients within Kachemak Bay.

> Hypothesis 2a: The surface nutrients in Kachemak Bay will reflect the results from Jakolof Bay where offshore water, groundwater, and river water all play a role in supplying macronutrients to the nearshore.
>
> Hypothesis 2b: As a reactive species, phosphate can adsorb to suspended solids in rivers and desorb in seawater, acting as an additional key source of phosphate previously uncharacterized in this region.

METHODS

Study Area

Kachemak Bay is in southcentral Alaska and connects to Cook Inlet and the NGA through a relatively narrow channel due to the presence of a spit, originally formed as a terminal glacial moraine, that separates inner and outer Kachemak Bay (Figure 1). Kachemak Bay derives its nutrients from (1) the Alaska Coastal Current which follows the NGA coastline before undergoing a slight excursion northward into Cook Inlet (Field and Walker, 2003; Stabeno et al., 2004), (2) a high rate of SGD (Lecher et al., 2016b; Haag, 2022), and (3) multiple rivers entering along its southern coast, fed by seven of the nine glaciers of the Harding Ice Field (Field and Walker, 2003).

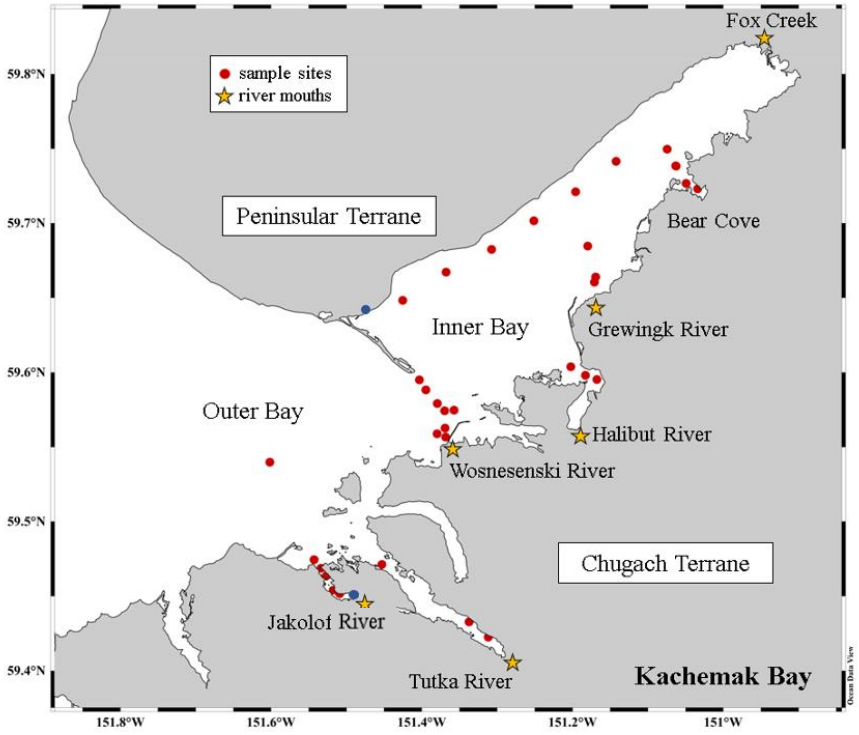

Figure 1: Map of Kachemak Bay; red dots are bay survey stations, blue dots are groundwater sample locations, and yellow stars are mouths of the rivers studied.

The buoyancy-driven estuary of inner Kachemak Bay creates a generally counter-clockwise circulation (Gatto, 1982; Johnson, 2021). The surface current along the south shore accumulates the glacial river discharge until the water reaches the extensive mudflats at the head of the bay. The water then exits inner Kachemak Bay along the shallow north side where the current reaches a maximum of 10 cm s^{-1} (Johnson, 2021). The flow of surface water through the narrow channel separating inner and outer Kachemak Bay changes seasonally depending on the state of river discharge. In winter, when freshwater runoff is low to negligible, floodwater can enter the inner bay following the bathymetry of the outer bay; however, there is generally little or no net circulation between the two bays (Gatto, 1982). In summer, the increased freshwater causes a net outflow through the narrow channel (Johnson, 2021) which stabilizes the inner bay circulation before the storm-driven autumn and winter mixing (Gatto, 1982).

Sampling and Analytical Methods

To determine the river Ra flux, six rivers in Kachemak Bay were sampled for ^{224}Ra, ^{226}Ra, and ^{228}Ra: Fox Creek, Jakolof River, Tutka River, Halibut River, Wosnesenski River, and Grewingk River. Due to fieldwork logistics, Fox Creek was sampled on May 18, 2021, while the others were sampled on July 10–11, 2021. July sampling occurred when the river discharge was greatest and more likely to obscure a groundwater Ra signal. We collected two 100 L Ra samples from each river: one as unaltered river water and a second salted to a salinity of 20 to achieve full desorption of Ra (Kelley et al., 2022). The water was filtered through MnO_2 fibers at < 2 L min^{-1} and counted on a Radium Delayed Coincidence Counter (RaDeCC) within two days at the Kasitsna Bay Laboratory. Three weeks later, the MnO_2 fibers were counted a second time at the University of Alaska Fairbanks to correct for ^{224}Ra supported by its parental isotope, ^{228}Th. Samples were then ashed at 800°C for 10 hours, sealed for three weeks, and counted for ^{226}R and ^{228}Ra on a gamma-ray spectrometer at the University of Hawaii at Manoa.

A Ra survey in Kachemak Bay covered the plumes of the major rivers, the narrow channel between inner and outer Kachemak Bay, and the shallow north side of inner Kachemak Bay (Figure 1) between July 12 and July 18, 2021. Large-volume surface seawater ^{224}Ra samples (> 100 L) were processed the same way as the river samples. Surface nutrient samples were also collected, filtered through a 0.45 µm nitrocellulose membrane filter, frozen in acid-cleaned HDPE bottles, and later thawed to analyze at the University of Alaska Fairbanks using a Seal Analytical continuous-flow QuAAtro39 AutoAnalyzer. On March 8, 2022, we ran a desorption experiment of phosphate from riverine-suspended solids at Jakolof River. In that experiment, triplicate nutrient samples were taken and adjusted to salinities of 0, 10, 20, and 30 using NaCl.

Discrete Ra groundwater samples were taken from the north (GPS 59.6385, -151.4800) and south (GPS 59.4503, -151.4874) sides of Kachemak Bay using a temporary PVC well See Figure 3 in Kelley et al., 2022). Sample volumes were >100 L. Logistics limited our ability to get more groundwater Ra samples.

Watershed Characteristics

The EPSCoR Fire and Ice program used satellite imagery to characterize physical and geomorphological characteristics (such as elevation, slope, area, forest area, wetland area, barren land area, lake area, and glacier area) of the study watersheds (Jordan Jenckes pers. comm.). These measures were used to examine the relationship between Ra concentration and watershed characteristics. Values were taken as a percentage of the entire watershed area they occupied. A Pearson correlation between the watershed characteristics and the Ra concentrations in the rivers resulted in no significant p-values, likely due to the small sample size employed.

RESULTS

Summer River Ra Signal

Every river in Kachemak Bay showed an increase in Ra concentration in the salted sample (shown as Total Ra in Figure 2). Taking the average values across all rivers, the exchangeable ^{224}Ra was five times greater than dissolved ^{224}Ra (4.97 to 6.08 dpm 100 L^{-1} and 0.37 to 1.83 dpm 100 L^{-1}, respectively). The exchangeable ^{226}Ra was seven times greater than dissolved ^{226}Ra (6.42 to 30.83 dpm 100 L^{-1} and 0 to 4.42 dpm 100 L^{-1}, respectively). The exchangeable ^{228}Ra was six times greater than dissolved ^{228}Ra (1.66 to 8.78 dpm 100 L^{-1} and 0 to 1.93 dpm 100 L^{-1}, respectively). The magnitude of this effect across all three Ra isotopes indicates that exchangeable Ra dominates the river Ra budget, and points to the importance of accounting for this fraction, which can desorb from the riverine suspended solids.

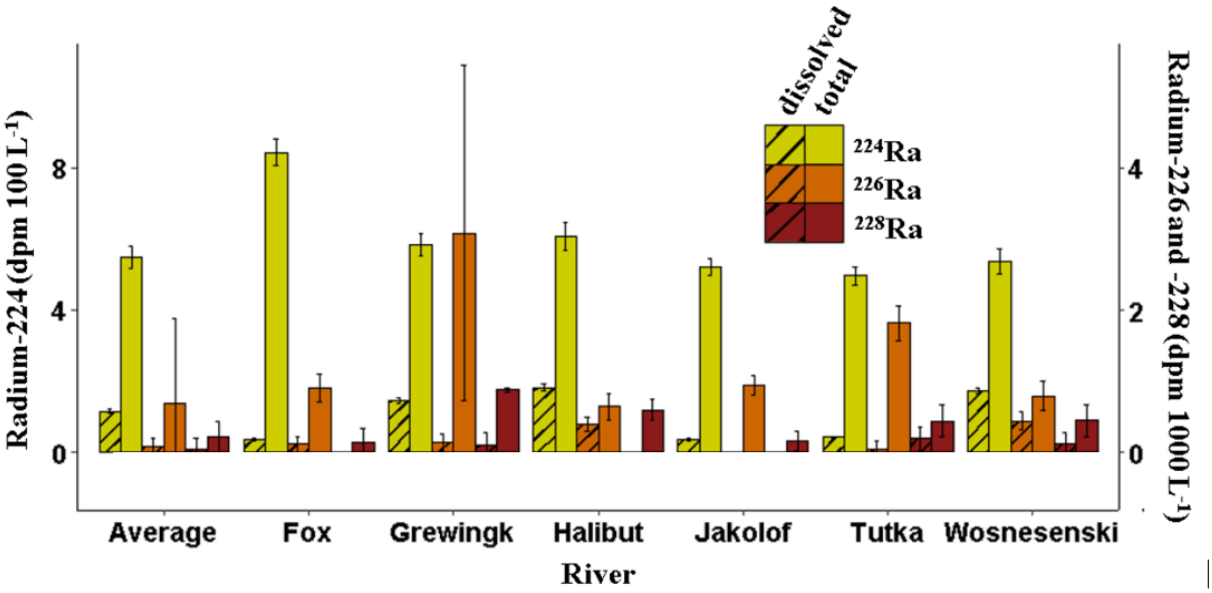

Figure 2: Dissolved and total (dissolved + exchangeable) Ra concentrations by river. Note that ^{224}Ra is scaled on the left axis, and ^{226}Ra and ^{228}Ra are scaled on the right axis. Error bars indicate the propagated error associated with the Ra measurement.

A modest relationship exists between dissolved ^{224}Ra and exchangeable ^{228}Ra (Table 1). The majority of the ^{228}Ra budget was the exchangeable fraction rather than the dissolved fraction (4.5 ± 2.7 dpm 100 L^{-1} and 0.71± 0.83 dpm 100 L^{-1}, respectively); therefore, it represents the

main source of ingrowth of 224Ra. When 228Ra adsorbed to the riverine suspended solids decays, its decay products, including 224Ra, undergo alpha recoil which always sends them into solution. This might explain the r2 of 0.71 between dissolved 224Ra concentration and exchangeable 228Ra concentration. It follows that there are relationships to mean elevation for both dissolved 224Ra concentration and exchangeable 228Ra concentration (r2 = 0.75 and r2 = 0.94, Table 1) since they are in the same decay chain.

Table 1: Correlations (r2) between the dissolved and exchangeable fractions of 224Ra, 226Ra, and 228Ra and watershed characteristics. Due to the small sample size (n = 6 rivers/watersheds), no correlations were significant (p > 0.05). Relationships greater than |0.75| are bolded.

Watershed Characteristics	**Dissolved [Ra]**			**Exchangeable [Ra]**		
	^{224}Ra	**^{226}Ra**	**^{228}Ra**	**^{224}Ra**	**^{226}Ra**	**^{228}Ra**
Dissolved [^{224}Ra]	-	**0.89**	0.06	-0.19	0.03	0.71
Dissolved [^{226}Ra]	-	-	-0.01	-0.01	-0.36	0.36
Dissolved [^{228}Ra]	-	-	-	-0.55	0.52	0.40
Exchangeable [^{224}Ra]	-	-	-	-	-0.21	-0.32
Exchangeable [^{226}Ra]	-	-	-	-	-	0.68
Exchangeable [^{228}Ra]	-	-	-	-	-	-
Watershed area	-0.17	0.12	-0.20	**0.84**	-0.24	-0.39
Max elevation	0.19	0.30	-0.20	**0.85**	0.04	0.08
Mean elevation	**0.75**	0.48	0.29	-0.03	0.57	**0.94**
Mean aspect	0.63	0.41	0.26	0.19	0.62	**0.82**
Mean slope	-0.59	-0.29	-0.22	**0.81**	-0.27	-0.59
Glacier %	0.57	0.27	0.28	0.05	0.73	**0.82**
Vegetation %	-0.62	-0.37	-0.61	0.18	0.70	**-0.91**
Forest %	-0.69	-0.56	-0.43	-0.02	-0.42	**-0.82**
Shrubland %	0.03	0.30	-0.53	0.22	**-0.82**	-0.40
Herbaceous %	-0.09	0.07	**0.84**	-0.52	-0.01	-0.04
Barren land %	0.12	0.23	0.71	-0.32	0.04	0.24
Open water %	0.31	-0.02	0.28	-0.07	**0.84**	0.70
Wetland %	0.29	0.04	-0.14	**0.75**	-0.31	-0.181

The longer-lived exchangeable Ra fractions were affected by the percentage of the watershed covered by glaciers (Jenckes et al., 2022). As mechanical erosion breaks up the bedrock at the glacier terminus, fine silt (glacial flour) is added to the river water. The bedrock geology was similar across all the rivers, which is evidenced by the exchangeable 226Ra concentration increasing linearly with the exchangeable 228Ra concentration (r2 = 0.68, Table 1). Higher glacial coverage in a watershed suggests relatively more glacial flour with this same geology is added to the river water. There was a positive relationship between percent glacial coverage and exchangeable 226Ra concentration (r2 = 0.73) as well as percent glacial coverage

and exchangeable ^{228}Ra concentration (r^2 = 0.82) (Table 1). These relationships were not observed for the exchangeable ^{224}Ra concentration (r^2 = 0.05), but that may be a result of sampling the rivers at different distances from their headwaters. Sampling locations at the river were chosen opportunistically based on trail access, so there could have been varying amounts of decay of the shorter-lived Ra ($t_{1/2}$ = 3.6 days) before sampling. With half-lives in the order of years, this issue would not affect measures for longer-lived Ra.

Exchangeable ^{224}Ra concentration was correlated with shorter-term processes. With the shortest half-life of the Ra isotopes, ^{224}Ra will reach equilibrium faster than its longer-lived counterparts. Therefore, the correlations between exchangeable ^{224}Ra concentration and watershed area (r^2 = 0.84), max elevation (r^2 = 0.85), mean slope (r^2 = 0.81), and wetland percent (r^2 = 0.75) indicate that these watershed characteristics affect short term processes.

Conversely, the longer-lived Ra isotopes were correlated with longer-term processes. There was still a partitioning between the watershed characteristics most closely associated with exchangeable ^{226}Ra concentration ($t_{1/2}$ = 1600 years) and exchangeable ^{228}Ra concentration ($t_{1/2}$ = 5.75 years). Exchangeable ^{228}Ra concentration was most closely correlated with mean elevation (r^2 = 0.94), mean aspect (r^2 = 0.82), vegetation percent (r^2 = -0.91), and forest percent (r^2 = -0.82) indicating that these are longer-term processes (Table 1). There were modest correlations between exchangeable ^{226}Ra concentration and these watershed characteristics, but they were weaker than the correlations with exchangeable ^{228}Ra concentration which might indicate that the ^{226}Ra requires more time to fully equilibrate. The processes correlated with exchangeable ^{226}Ra concentration must be even longer-term than the ones associated with exchangeable ^{228}Ra concentration: shrubland percent (r^2 = -0.82) and open water percent (r^2 = 0.84). Exchangeable ^{228}Ra concentrations had weaker correlations to these characteristics, though they were still modest (Table 1).

Summer Groundwater Ra Signal

The groundwater Ra flux on the south side of Kachemak Bay was masked by the river Ra discharge. Bear Cove, a semi-enclosed embayment that does not contain a significant river source, showed a linear decrease in ^{224}Ra concentration toward the head of the cove (r^2 = 0.997). This indicates that the dominant source of ^{224}Ra was from Kachemak Bay and that this concentrated Ra signal mixed conservatively with the cove water (Lecher et al., 2016a). The surface salinity decreased linearly going into the cove (r^2 = 0.895) indicating a source of terrestrial freshwater inside Bear Cove such as numerous small creeks, fresh groundwater, or runoff. However, our results indicate that ^{224}Ra cannot be used as a tracer for groundwater in this cove because the accumulated river ^{224}Ra signal along the south side of Kachemak Bay overwhelms the ^{224}Ra groundwater flux and accumulated freshwater inputs from within Bear Cove.

The groundwater Ra concentration was lower on the south side of Kachemak Bay than on the north side (Figure 3). Compared to southern groundwater [Ra], the northern groundwater ^{224}Ra concentration was twelve times greater, the ^{226}Ra concentration was five times greater, and the ^{228}Ra concentration was twelve times greater. The magnitude of difference in the Ra

concentration on the north and south side for ^{224}Ra and ^{228}Ra was similar since they are in the same decay chain; therefore, if one is greater, it follows that the other is as well. The salinity of the groundwater on the south side was 2.6 whereas the groundwater salinity on the north side was 20.2, which means full desorption of Ra from the aquifer sediments had not yet occurred in the southern groundwater. Using the linear desorption of ^{224}Ra to salinity reported by Kelley et al. (2022), the maximum groundwater ^{224}Ra concentration on the south side could be estimated as high as 20 dpm 100 L^{-1}. Under this scenario, the southern groundwater ^{224}Ra concentration was three times less concentrated than the north side. Since the north side has a higher groundwater Ra concentration and no major rivers passing through the geology, we could detect a groundwater Ra signal in seawater.

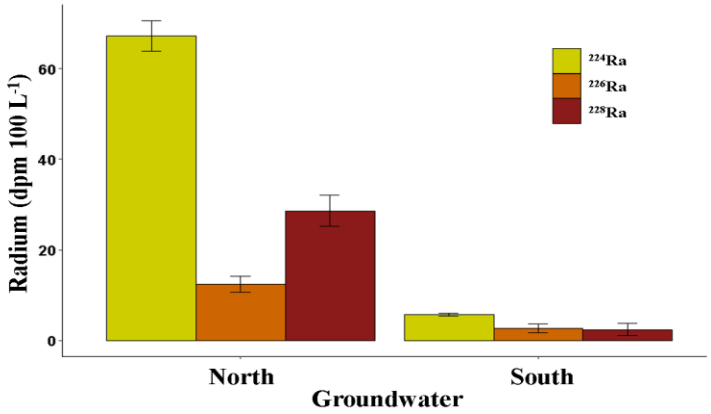

Figure 3: Concentrations of Ra isotopes dissolved in groundwater on the north and south side of Kachemak Bay. Error bars indicate the propagated error associated with the Ra measurement.

An observed ^{224}Ra enrichment in seawater on the north side of Kachemak Bay (Figure 4) was likely a groundwater signal. The seawater ^{224}Ra concentration in the river plumes on the south side of Kachemak Bay did not exceed 3.6 dpm 100 L^{-1}, but the seawater ^{224}Ra concentration along the transect on the shallow north side ranged from 4.4 – 6.6 dpm 100 L^{-1} (average = 5.5 dpm 100 L^{-1}, SD = 0.73 dpm 100 L^{-1}, n=7) (Figure 4). This water might be influenced by Sheep Creek and Fox Creek discharging into the head of the bay. However, the total ^{224}Ra concentration in Fox Creek (8.8 dpm 100 L^{-1}) was in the ^{224}Ra concentration range for rivers on the south side of Kachemak Bay (Figure 2) and those rivers did not raise the seawater ^{224}Ra concentration past 3.6 dpm 100 L^{-1}. Mudflats). Present at the head of the bay, mudflats, which can facilitate high SGD (Haag, 2022), are a likely source of the higher ^{224}Ra concentrations observed on the north side of the inner Kachemak Bay. However, the highest ^{224}Ra concentration on the north side transect was 25 km from the head of the bay, suggesting another source halfway down the bay. Therefore, river discharge does not completely mask the groundwater ^{224}Ra signal from the north side of the bay.

SGD diffuses heterogeneously along the north side of inner Kachemak Bay. While the high ^{224}Ra concentration is continuous along the length of the north side, the highest seawater ^{224}Ra concentration occurs concurrently with an increase in current speed (Johnson, 2021; Figure

5). As the current increases in speed, there is a divergence in the water column which, in deeper water, would create upwelling. In this case, it may allow for greater SGD as the divergence pulls porewater from the sediment. A profile of the water column along this transect (see red box in Figure 4) reveals a less dense, fresher, and warmer water mass at the same location of the high ^{224}Ra, all indicators of SGD (Figure 5). The inversion of denser water between this water mass and the river plume from Fox Creek indicates that it is a separate water mass and that this signal is likely SGD.

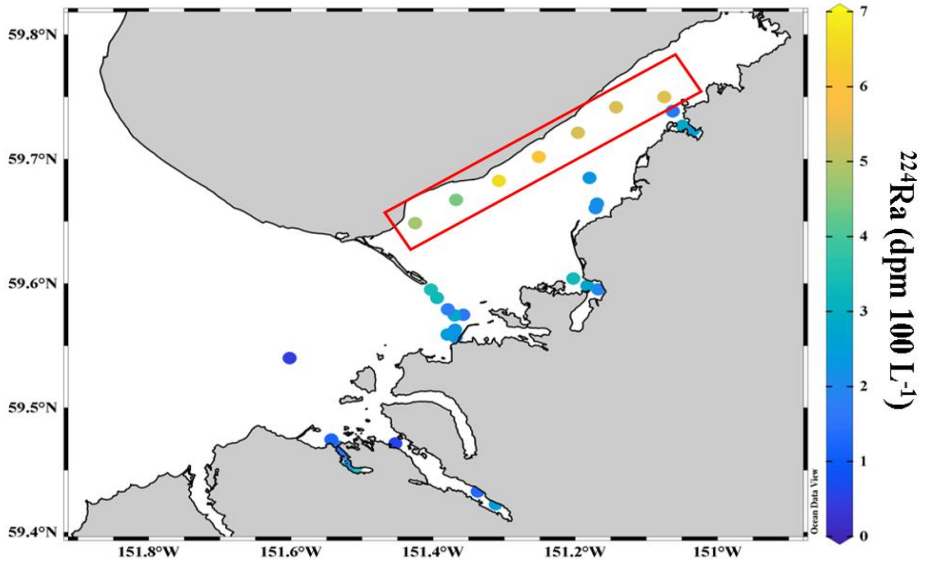

Figure 4: ^{224}Ra concentration in seawater surface (~0.5 m depth) in Kachemak Bay. The red box indicates the transect conducted on the north side of inner Kachemak Bay.

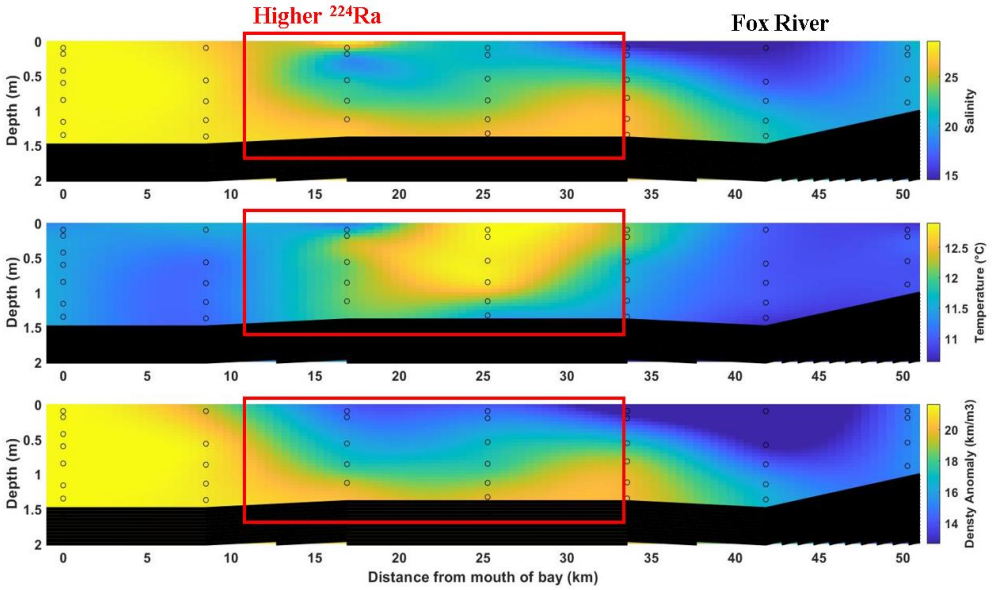

Figure 5: Profile of the water column along the north side of Kachemak Bay. The red boxes indicate the highest ^{224}Ra detected in the surface seawater of Kachemak Bay.

Distribution of Nutrients in Kachemak Bay

Despite decades of oceanographic research in Kachemak Bay, it remains unclear whether the primary source of nutrients fueling coastal food webs is the offshore waters advected in from the Alaska Coastal Current or localized inputs from land-based sources (i.e., rivers and groundwater). In the semi-enclosed Jakolof Bay, where there is minimal river discharge, groundwater and offshore water compete as the primary source of nitrate (NO_3^-), groundwater is the primary source of silicic acid ($Si(OH)_4$), and offshore water and river water are sources of phosphate (PO_4^{3-}) (Haag, 2022).

The surface seawater nutrient samples taken during the Kachemak Bay survey (Figure 6) agree in large part with the Jakolof Bay nutrient distribution. The NO_3^- concentration and ammonium (NH_4^+) do not follow a relationship with salinity ($r^2 = 0.01$ and $r^2 = 0.00$, respectively). As NO_3^- is the limiting nutrient in coastal seawater (Figure 6) and NH_4^+ is the most energetically efficient form of bioavailable N, any NO_3^- or NH_4^+ in excess is readily taken up for primary production. Fresher seawater (river water, brackish groundwater, and/or runoff) contains higher N:P than saline seawater (offshore water, saline groundwater) ($r^2 = 0.46$). This is due to saline water being a greater source of PO_4^{3-} than fresh water ($r^2 = 0.37$, Figure 6). Aquifers act as a sink for PO_4^{3-} (Lecher et al., 2016b); therefore, the PO_4^{3-} input from saline water likely represents the offshore water.

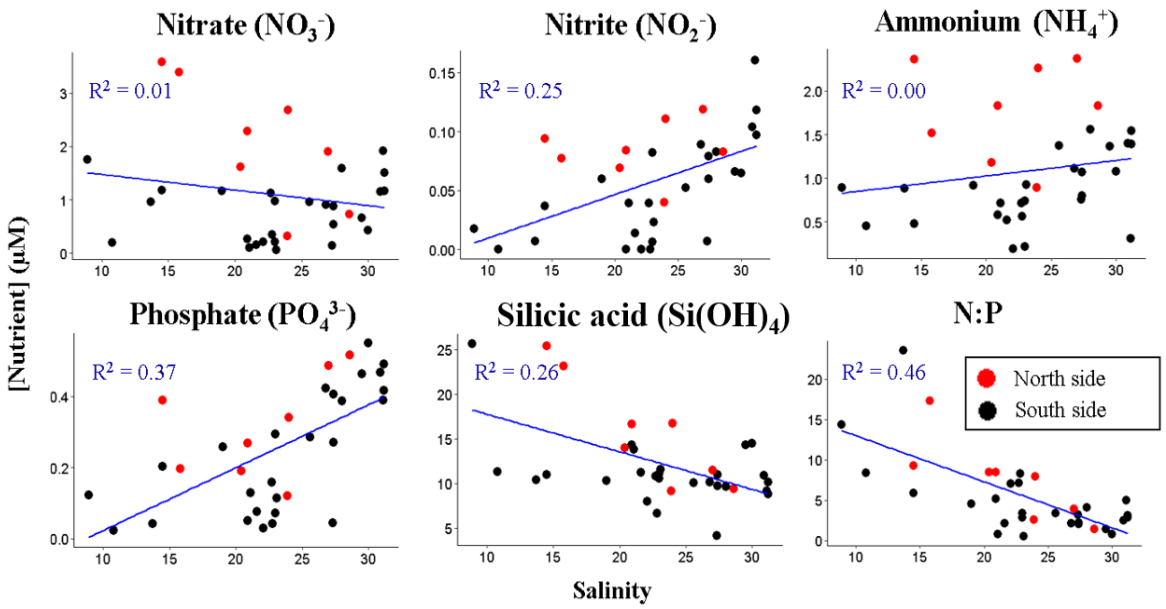

Figure 6: Kachemak Bay survey nitrate, nitrite, ammonium, phosphate, and silicic acid concentrations and N:P ratios at increasing salinities.

The surface seawater on the north side of Kachemak Bay had high concentrations of NO_3^-, NH_4^+, and $Si(OH)_4$ (Figure 6). This shallow stretch of water (~1.5 m depth) experiences the highest currents in Kachemak Bay (>6 cm s^{-1}, Johnson, 2021), accumulated glacier river discharge, and groundwater discharge. In addition, a strong current can resuspend sediment,

allowing for nutrient diffusion from these particles. The higher NO_3^- and NH_4^+ concentrations observed (forms of N that are limiting in coastal waters) suggest that nutrients are not readily taken up by primary production on the north side of Kachemak.

Rivers as a Source of Phosphate

Raising the salinity of Jakolof Creek water samples using NaCl did not result in linear desorption of phosphate from riverine-suspended solids as was previously observed for Ra (Kelley et al., 2022). Even though the triplicates for the phosphate at each salinity treatment in the desorption experiment were taken from a single sample, the variation in [PO_4^{3-}] measured resulted in a poor linear regression with a p-value > 0.05 and a r^2 of 0.05 (Figure 7). The error associated with the triplicate samples ranged from 5 % to 56 % indicating that the NaCl used in the experiment was contaminated with PO_4^{3-} or not enough time was allowed for the equilibrium of PO_4^{3-} desorption from the riverine suspended solids. We allowed one minute for the PO_4^{3-} to desorb before running the first sample, but subsequent replicates had additional time for desorption to occur while they waited. However, since the error for the triplicate with no NaCl added (and no equilibrium reached) was 16 %, that sample did not follow either of the possibilities described above. This experiment might show natural variability of the PO_4^{3-} concentration in the river water, but we cannot draw conclusive information from this experiment.

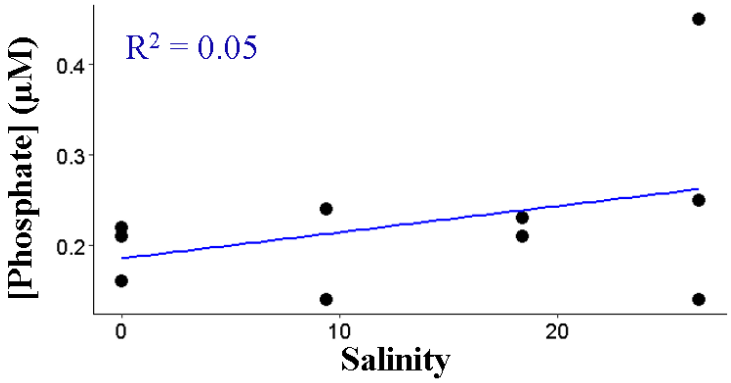

Figure 7: Phosphate desorbed from riverine particles from the Jakolof River at increasing salinities. This linear relationship has an r^2 = 0.05 and a p-value > 0.05.

DISCUSSION

This work presents the radium (Ra) and nutrients within Kachemak Bay during the summer of 2021. However, the discharge from all six rivers varies over time, due to rainfall in autumn and early spring, and peak glacial melt in late summer (Jenckes et al., 2022), therefore the influence of the rivers will vary in other seasons. As the discharge of glacier-fed river water into Kachemak Bay decreases in winter, we might be able to detect groundwater Ra. However, as the river discharge decrease and the transit time of river water from headwaters to seawater slows, the Ra concentration might increase following the typical concentration-discharge pattern seen in other places around the world. In the NGA, Jenckes et al. (2022) found that watershed characteristics and glacier coverage play major roles in determining the amount of solute that can

be introduced to a river. We observed similar findings with respect to Ra in this project. Further research in other seasons must be conducted to fully understand the utility of Ra-based approaches in this region based on the changing flow regime of rivers as well as ocean currents.

The variables that need to be considered when applying these results to other locations within Cook Inlet are underlying geology and river discharge. Bear Cove, a semi-enclosed inlet with offshore waters enriched in ^{224}Ra due to the high amount of glacial river discharge in the region, does not have a noticeable groundwater ^{224}Ra signal. Jakolof Bay, another semi-enclosed bay along the south side of Kachemak Bay, is located outside the influence of large river plumes and a groundwater ^{224}Ra signal is detected there (Kelley et al., 2022). Another groundwater signal is detected on the north side of inner Kachemak Bay where the geology is different, allowing the groundwater ^{224}Ra concentration to be greater than on the south side. Without appreciable river discharge on the north side, the groundwater ^{224}Ra signal is greater than the background seawater ^{224}Ra concentration along an open coastline. This demonstrates the ability of river discharge to mask a groundwater ^{224}Ra signal when both sources of water originate from within the same geology.

The seawater enriched in ^{224}Ra concentration exiting Kachemak Bay is quickly depleted in the tracer as it decays and mixes with less concentrated offshore water. The water exiting the inner bay by Homer has a surface seawater ^{224}Ra concentration of 3.4 dpm 100 L^{-1} and approximately 12 km farther into the outer Kachemak Bay the surface seawater ^{224}Ra concentration is 0.4 dpm 100 L^{-1}. Water samples taken away from the coastline are likely to be highly depleted in ^{224}Ra, with potential "hotspots" only occurring in the presence of a shallow bank where sediments are mixed into the water column and desorb ^{224}Ra (Burt et al., 2013; Kandel and Aguilar-Islas, 2021), an offshore spring where groundwater ^{224}Ra is released, or other natural or human-introduced discharges carrying detectable short-lived Ra signals compared to seawater's short-lived Ra concentration.

ACKNOWLEDGMENTS

This project was accomplished at the University of Alaska Fairbanks Troth Yeddha' campus, which was established on the traditional homelands of the Lower Tanana Dené. I conducted this research as a guest working on these unceded lands of the Dena'ina and Alutiiq peoples. I am grateful to the Kasitsna Bay laboratory staff for their assistance on this project and to the EPSCoR Fire and Ice Project, and many of its members, including Dr. LeeAnn Munk, Jordan Jenckes, and Dr. Katrin Iken for supporting this work. Thank you to Dr. Amanda Kelly and Dr. Ana Aguilar-Islas and laboratory team members Marina Alcantar, Shelby Bacus, James Currie, and Jonah Jossart. This project was funded through the Alaska Coastal Marine Institute by the U.S. Department of the Interior, Bureau of Ocean Energy Management, under cooperative agreement M20AC10016, principal investigators William Burt and Amanda Kelley.

REFERENCES

Archer, A. W. 2013. World's highest tides: Hypertidal coastal systems in North America, South America, and Europe. Sedimentary Geology, 284:1–25.

Bradley, D. C., Kusky, T. M., Haeussler, P. J., Karl, S. M., and Donley, D. T. 1999. Geologic Map of the Seldovia Quadrangle, South-central Alaska. U.S. Geological Survey Open-File Report OFR 99-18B.

Burt, W. J., Thomas, H., and Auclair, J. P. 2013. Short-lived radium isotopes on the Scotian Shelf: Unique distribution and tracers of cross-shelf CO2 and nutrient transport. Marine Chemistry, 156:120–129.

Croff, C., Lessman, J., Bigelow, C., and Ruzicka, J. 1977. Uranium Favorability of the Cook Inlet Basin, Alaska. U.S. Department of Energy Office of Science and Technology, Technical Report No. GJBX-41 (78):V1. WGM, Inc., Anchorage, AK. doi:10.2172/6538411.

Dickinson, K. A., and Campbell, J. A. 1978. Epigenetic Mineralization and Areas Favorable for Uranium Exploration in Tertiary Continental Sedimentary Rock in South-central Alaska: A Preliminary Report. U.S. Geological Survey, Open File Report 78-757. doi:10.3133/ofr78757.

Field, C.M., and Walker, C. 2003. A Site Profile of the Kachemak Bay Research Reserve, a Unit of the National Estuarine Research Reserve System. Kachemak Bay Research Reserve, Homer, AK. https://coast.noaa.gov/data/docs/nerrs/Reserves_KBA_SiteProfile.pdf.

Garcia-Orellana, J., Rodellas, V., Tamborski, J., Diego-Feliu, M., van Beek, P., Weinstein, Y., ... and Scholten, J. 2021. Radium isotopes as submarine groundwater discharge (SGD) tracers: Review and recommendations. Earth-Science Reviews, 220, 103681.

Gatto, L. W. 1982. Ice distribution and winter surface circulation patterns, Kachemak Bay, Alaska. Remote Sensing of Environment, 12(5):421–435.

Haag, J. 2022. The utility of radium as a tracer in a river-dominated system. In preparation.

Hancock, G. J., and Murray, A. S. 1996. Source and distribution of dissolved radium in the Bega River estuary, Southeastern Australia. Earth and Planetary Science Letters, 138(1–4): 145–155.

Hancock, G. J., Webster, I. T., and Stieglitz, T. C. 2000. Horizontal mixing of Great Barrier Reef waters: Offshore diffusivity determined from radium isotope distribution. Journal of Geophysical Research: Oceans, 111(C12).

Jenckes, J., Ibarra, D. E., and Munk, L. A. 2022. Concentration-discharge patterns across the Gulf of Alaska reveal geomorphological and glacierization controls on stream water solute generation and export. Geophysical Research Letters, 49(1), e2021GL095152.

Johnson, M. A. 2021. Subtidal surface circulation in lower Cook Inlet and Kachemak Bay, Alaska. Regional Studies in Marine Science, 41:101609.

Kandel, A., and Aguilar-Islas, A. 2021. Spatial and temporal variability of dissolved aluminum and manganese in surface waters of the northern Gulf of Alaska. Deep Sea Research Part II: Topical Studies in Oceanography, 189:104952.

Kelley, A., Burt, W., and Haag, J. 2022. Exploring radium isotopes as tracers of groundwater inputs and flushing rates in Cook Inlet, Alaska. Final Report, OCS Study BOEM 2022-045, Alaska Coastal Marine Institute and USDOI, BOEM Alaska OCS Region.

Lecher, A. L., Kessler, J., Sparrow, K., Garcia-Tigreros Kodovska, F., Dimova, N., Murray, J., ... and Paytan, A. 2016a. Methane transport through submarine groundwater discharge to the North Pacific and Arctic Ocean at two Alaskan sites. Limnology and Oceanography, 61(S1):S344–S355.

Lecher, A. L., Chien, C. T., and Paytan, A. 2016b. Submarine groundwater discharge as a source of nutrients to the North Pacific and Arctic coastal oceans. Marine Chemistry, 186:167–177.

Moore, W. S. 2000. Determining coastal mixing rates using radium isotopes. Continental Shelf Research, 20(15):1993–2007.

Oey, L. Y., Ezer, T., Hu, C., and Muller-Karger, F. E. 2007. Baroclinic tidal flows and inundation processes in Cook Inlet, Alaska: numerical modeling and satellite observations. Ocean Dynamics, 57(3):205–221.

Pavlis, T. L., Roeske, S. M., Ridgway, K. D., Trop, J. M., Glen, J. M. G., and O'Neill, J. M. 2007. The Border Ranges fault system, southern Alaska. Special Papers-Geological Society of America, 431:95.

Plafker, G., Nokleberg, W. J., and Lull, J. S. 1989. Bedrock geology and tectonic evolution of the Wrangellia, Peninsular, and Chugach terranes along the Trans-Alaska Crustal Transect in the Chugach Mountains and southern Copper River Basin, Alaska. Journal of Geophysical Research: Solid Earth, 94(B4):4255–4295.

Santos, I. R., Chen, X., Lecher, A. L., Sawyer, A. H., Moosdorf, N., Rodellas, V., ... and Li, L. 2021. Submarine groundwater discharge impacts on coastal nutrient biogeochemistry. Nature Reviews Earth and Environment, *2*(5):307–323.

Schmoll, H. R., Yehle, L. A., Gardner, C. A., and Odum, J. K. 1984. Guide to Surficial Geology and Glacial Stratigraphy in the Upper Cook Inlet Basin: Anchorage. Alaska Geological Society. https://ngmdb.usgs.gov/Prodesc/proddesc_89397.htm.

Sharp, J. M., Jr. 1984. Hydrogeologic characteristics of shallow glacial drift aquifers in dissected till plains (north-central Missouri). Groundwater, 22(6):683–689.

Sharp, J. M., Jr.1988. Alluvial aquifers along major rivers. pp. 273–.282 in Hydrology (Back, W., Rosenshein, J. S., and Seaber, P. R., eds.), The Geology of North America. Geological Society of America, Boulder, CO.

Stabeno, P. J., Bond, N. A., Hermann, A. J., Kachel, N. B., Mordy, C. W., and Overland, J. E. 2004. Meteorology and oceanography of the Northern Gulf of Alaska. Continental Shelf Research, 24(7–8):859–897.

Tranter, M. 1982. Controls on the Chemical Composition of Alpine Glacial Meltwaters. Doctoral dissertation, University of East Anglia, uk.bl.ethos.331807.

Tranter, M. 2003. Geochemical weathering in glacial and proglacial environments. Treatise on Geochemistry, 5:605.

The Department of the Interior Mission

As the Nation’s principal conservation agency, the Department of the Interior has responsibility for most of our nationally owned public lands and natural resources. This includes fostering the sound use of our land and water resources, protecting our fish, wildlife and biological diversity; preserving the environmental and cultural values of our national parks and historical places; and providing for the enjoyment of life through outdoor recreation.The Department assesses our energy and mineral resources andworks to ensure that their development is in the best interests of all our people by encouraging stewardship and citizen participation in their care. The Department also has a major responsibility for American Indian reservation communities and for people who live in island communities.

The Bureau of Ocean Energy Management

The Bureau of Ocean Energy Management (BOEM) works to manage the exploration and development of the nation's offshore resources in a way that appropriately balances economic development, energy independence, and environmental protection through oil and gas leases, renewable energy development and environmental reviews and studies.